JACS
JOURNAL OF THE AMERICAN CHEMICAL SOCIETY
pubs.acs.org/JACS
Communication

Dissecting Electronic-Structural Transitions in the Nitrogenase MoFe Protein P-Cluster during Reduction

Bryant Chica, Jesse Ruzicka, Lauren M. Pellows, Hayden Kallas, Effie Kisgeropoulos, Gregory E. Vansuch, David W. Mulder, Katherine A. Brown, Drazenka Svedruzic, John W. Peters, Gordana Dukovic, Lance C. Seefeldt, and Paul W. King*

Cite This: J. Am. Chem. Soc. 2022, 144, 5708–5712
Read Online
ACCESS | Metrics & More | Article Recommendations | Supporting Information

ABSTRACT: The [8Fe-7S] P-cluster of nitrogenase MoFe protein mediates electron transfer from nitrogenase Fe protein during the catalytic production of ammonia. The P-cluster transitions between three oxidation states, P^N, P^+, P^{2+} of which $P^N \leftrightarrow P^+$ is critical to electron exchange in the nitrogenase complex during turnover. To dissect the steps in formation of P^+ during electron transfer, photochemical reduction of MoFe protein at 231−263 K was used to trap formation of P^+ intermediates for analysis by EPR. In complexes with CdS nanocrystals, illumination of MoFe protein led to reduction of the P-cluster P^{2+} that was coincident with formation of three distinct EPR signals: $S = 1/2$ axial and rhombic signals, and a high-spin $S = 7/2$ signal. Under dark annealing the axial and high-spin signal intensities declined, which coincided with an increase in the rhombic signal intensity. A fit of the time-dependent changes of the axial and high-spin signals to a reaction model demonstrates they are intermediates in the formation of the P-cluster P^+ resting state and defines how spin-state transitions are coupled to changes in P-cluster oxidation state in MoFe protein during electron transfer.

Nitrogenase is a two-component enzyme that catalyzes the conversion of dinitrogen to ammonia. Under ideal reaction conditions, the Mo-dependent form of nitrogenase, composed of Fe protein and MoFe protein, catalyzes N_2 reduction to ammonia according to eq 1:[1]

$$N_2 + 8e^- + 8H^+ + 16ATP \rightarrow 2NH_3 + H_2 + 16ADP + 16P_i \quad (1)$$

During turnover, the electrons required for N_2 reduction are transferred from Fe protein to MoFe protein, which is an $\alpha_2\beta_2$ tetramer that coordinates two sets of unique metal clusters. The [8Fe-7S] P-cluster functions in electron transfer with Fe protein, and the [7Fe-9S-1Mo-C-Homocitrate] iron−molybdenum cofactor (FeMo-co) functions as the site of N_2 reduction.[2]

One of the unique aspects of how nitrogenase catalyzes ammonia production is the electron transfer process.[3,4] In the catalytic cycle, the P-cluster forms a metastable intermediate oxidation state, P^+ ($[7Fe^{II}Fe^{III}\text{-}7S]^{+1}$), that is rapidly reduced ($k > 1700\ s^{-1}$)[3] during electron transfer. In addition to P^+, the P-cluster forms two stable oxidation states, P^N ($[8Fe^{II}\text{-}7S]^0$ and P^{2+} ($[6Fe^{II}2Fe^{III}\text{-}7S]^{+2}$) (Figure 1).[5] Transitions between P-cluster states involve extensive structural changes, including a switch in Fe-coordination of the central sulfide (S_1) that bridges the two [4Fe-3S] subclusters, and amide nitrogen coordination to Fe_S by α-88 cysteine (α-88Cys) and β-188 serine (β-188Ser) oxygen coordination to Fe_6. Recently, the X-ray structure of MoFe protein was solved with the P-cluster poised in the P^+ state, with an intermediate structural arrangement between P^{2+} and P^N (Figure 1).[6] In the P^+ state, the S_1 sulfide is pentacoordinate and β-188Ser coordinates Fe_6. The observation of structural changes in the MoFe protein P-cluster has been incorporated into conformational gating[7] and mechanical coupling[8,9] electron transfer models. The model predicts that motions near the P-cluster and β-188Ser are coupled to "switch regions" in the Fe protein that steer structural interactions within the nitrogenase complex to enable electron delivery.[9]

The structural rearrangements of the P-cluster in different oxidation states also coincide with changes in spin states and EPR properties. P^{2+} is an integer spin state, likely $S = 4$, and gives rise to an EPR signal at $g = 11.8$,[10,11] whereas P^N is an $S = 0$ spin state and EPR-silent. The P^+ oxidation state has a rhombic, $S = 1/2$ EPR signal at $g = 2.05, 1.94, 1.81$ that shifts to $g = 2.03, 1.97, 1.93$ when β-188Ser is substituted by Cys.[12,13] Additional magnetic signals associated with the P^+ oxidation state include an $S = 1/2$ signal with $g = 2.00$ and 1.89,[13,14] and low-field $S = 5/2$ signals[12,13] (Table S1). Variations in P^+ magnetic states have been observed in MoFe protein under different redox titration conditions (Table S2).[13−15] Whether these states have a functional role in electron transfer in MoFe protein remains unclear. Recently, the structural and magnetic configurations of the P-cluster oxidation states were shown to coincide with profound

Received: December 17, 2021
Published: March 22, 2022

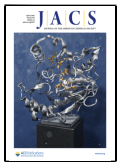

https://doi.org/10.1021/jacs.1c13311
J. Am. Chem. Soc. 2022, 144, 5708−5712

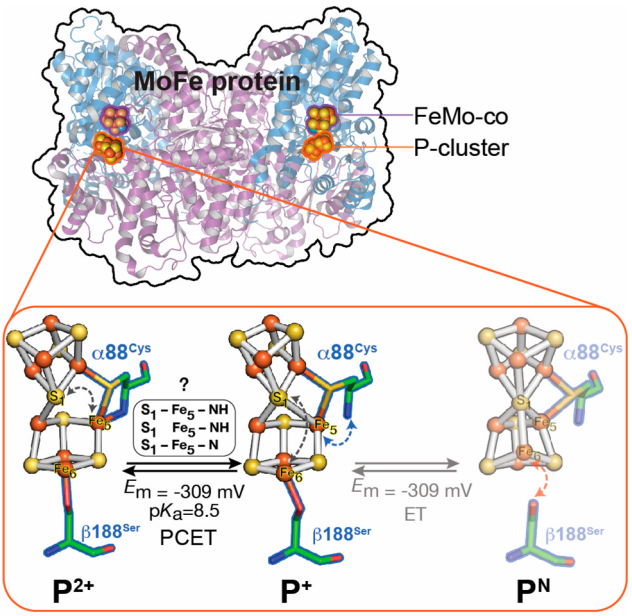

Figure 1. MoFe protein P-cluster oxidation state structures for P^{2+}, P^{+}, and P^{N}. The α-88^{Cys} ($P^{2+}\leftrightarrow P^{+}$) and β-188^{Ser} ($P^{+}\leftrightarrow P^{N}$) ligands that undergo redox-coupled coordination changes to the P-cluster are shown. The $P^{2+}\leftrightarrow P^{+}$ transition involves exchange of the S_1-Fe_5 thiolate bond (gray arrow) and α-88^{Cys} amide bond at Fe_5 (blue arrow) and proceeds via proton-coupled electron transfer (PCET), where changes in bonding (box) may lead to different conformers during electron transfer. The $P^{+}\leftrightarrow P^{N}$ transition involves exchange of the S_1-Fe_6 thiolate bond and β-188^{Ser} serine hydroxylate bond at Fe_6 (red arrow). E_m = −309 mV at pH 8 for both transitions.[11] PDB Codes: P^{2+}, 2MIN; P^{+}, 6CDK; P^{N}, 3MIN.

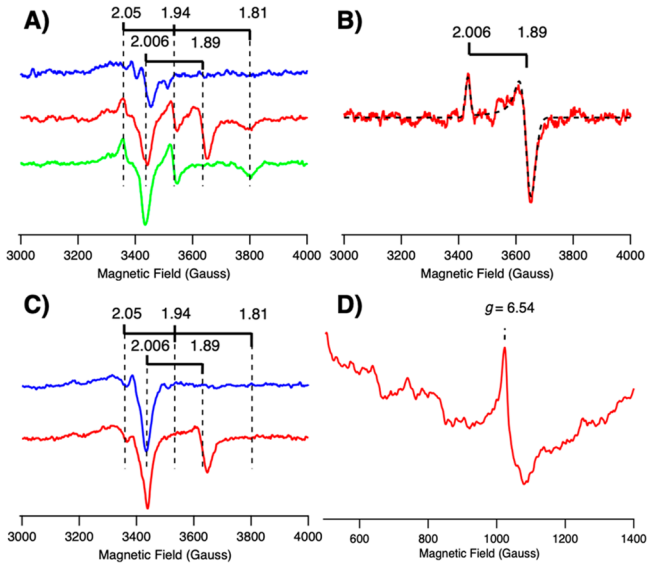

Figure 2. Illumination and EPR spectra of CdS:MoFe protein complexes at 263 K and 231 K. (A) T = 263 K. Blue trace, oxidized CdS:MoFe protein complexes. Red trace, after 12 min illumination at 263 K. Green trace, spectrum after incubation in the dark at 263 K for 20 min. (B) Illuminated (red trace) minus dark (green trace) difference spectrum. Simulation (black dashed trace) using g = 2.006, 1.89 assigned to the S = 1/2, $P^{+}_{1.89}$ signal. Buffer pH = 7; EPR conditions, T = 12 K, microwave power = 1 mW. (C) T = 231 K. Blue trace, oxidized CdS:MoFe protein complexes. Red trace, after 15.5 min illumination at 231 K. (D) Low-field EPR spectrum showing the high-spin, S = 7/2, g = 6.54 signal assigned as $P^{+}_{6.54}$. Sample pH = 7. EPR conditions: (C) T = 12 K, microwave power = 1 mW, (D) T = 18 K, microwave power = 25 mW. Populations of EPR signals are summarized in Table S1.

differences in the density of low lying electronic states, implying there is a deeper relationship between the electronic-structural properties of the P-cluster and its function in electron transfer.[10]

Resolving the relationship between the magnetism and structure of the P-cluster, most notably for the metastable P^{+} state, is important for elucidating a complete mechanistic understanding of the P-cluster in the nitrogenase electron transfer cycle. Herein, we address this goal by combining light-controlled reduction of MoFe protein in complexes with cadmium sulfide nanocrystals (CdS)[16,17] with EPR to resolve magnetic changes in the P-cluster during electron transfer that arise from discrete electronic-structural intermediates in the reduction of P^{2+} to P^{+}.

An oxidized sample of nitrogenase MoFe protein was mixed with mercaptopropionic acid capped CdS quantum dots (Figure S1; see Supporting Information for details), and the P-cluster P^{2+} oxidation state was verified by EPR (Figure S2). The CdS:MoFe protein complexes were illuminated with a 405 nm LED at either 231 K or 263 K and then allowed to anneal in the dark at 236 K or 263 K, respectively, to prevent further light-driven reduction. By illuminating at subambient temperatures, the light-driven redox (i.e., electron transfer) process is decoupled from temperature sensitive chemical (i.e., ligand switching) steps during electron transfer and P-cluster conversion from $P^{2+}\leftrightarrow P^{+}$. As shown in Figure 2A, illumination at 263 K for 12 min resulted in reduction of the P-cluster exemplified by loss of P^{2+} intensity (36%, Figure S2 and Table S1). This change coincided with the appearance of an S = 1/2 rhombic signal at g = 2.05, 1.94, 1.81 ($P^{+}_{1.81}$, Figure 2A)[13,15,18] and an S = 1/2 axial signal with g = 2.006, 1.89 (assigned to $P^{+}_{1.89}$, Figure 2B).[13,14] Dark annealing at 263 K for 20 min (Figure 2A, green trace) led to complete loss of the $P^{+}_{1.89}$ signal, and an increase in amplitude of the $P^{+}_{1.81}$ (21%) and P^{2+} (7%) signals (Table S1).

When illuminated at a lower temperature of 231 K for 15.5 min, reduction of the MoFe protein P-cluster led to a decrease in the P^{2+} signal intensity (19%) and appearance of the $P^{+}_{1.89}$ signal, whereas formation of the $P^{+}_{1.81}$ signal was suppressed. Rather, a low-field inflection at g = 6.54 (Figure 2D) appeared, resembling other high-spin signals observed for MoFe protein (Table S2, Figure S3). Rhombogram analysis and simulation of the g = 6.54 signal (referred to as $P^{+}_{6.54}$) indicates that it originates from a S = 7/2 spin system with E/D ≈ 0.024 (D = −3.2 cm^{-1}) of the reduced P-cluster, where E and D[19] are the zero-field splitting parameters (see Figure S3 for details).

Dark annealing at 236 K of the CdS:MoFe protein complexes illuminated at 231 K (Figure 2C) was used to monitor relative intensities of P^{+} intermediates following light-driven electron transfer to MoFe protein (Figure S4). EPR spectra of CdS or MoFe protein alone, before and after illumination and annealing, or of CdS:MoFe protein prior to illumination, did not produce any detectable signal changes (Figure S5). Simulations of the low-field regions using singular value decomposition (SVD, Figure S6) and the high-field region using EasySpin[20] (Table S3, Figure S7) enabled time-dependent changes in signal intensities of P^{+} intermediates ($P^{+}_{1.89}$, and $P^{+}_{1.81}$ and $P^{+}_{6.54}$) to be fit to reaction models (Tables S4 and S5, Figure S8). The P^{+} signal intensity versus

https://doi.org/10.1021/jacs.1c13311
J. Am. Chem. Soc. 2022, 144, 5708−5712

annealing time best fit to a three-step reaction model as summarized in eqs 2 and 3:

$$P^{+}_{6.54} \xrightarrow{k_1} P^{+}_{1.89} \xrightarrow{k_3} P^{+}_{1.81} \quad (2)$$

$$P^{+}_{6.54} \xrightarrow{k_2} P^{+}_{1.81} \quad (3)$$

The fit shown in Figure 3 gave relative values for rate constants where $k_2 > k_1 > k_3$ and predicts the high-spin $P^{+}_{6.54}$

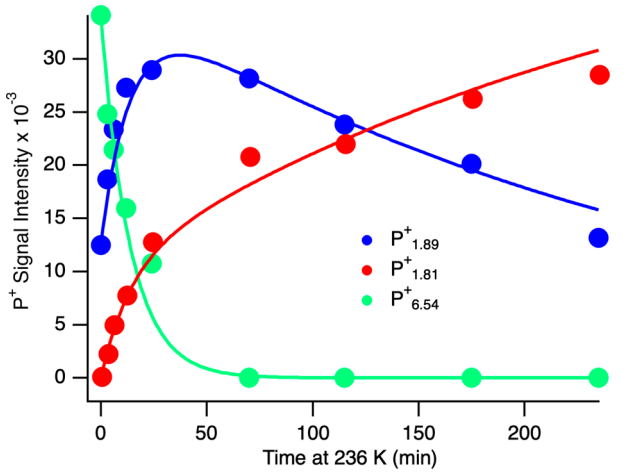

Figure 3. Time-dependent changes of the P^{+} EPR signals intensities in CdS:MoFe protein complexes. Initial (time = 0 min) P^{+} signal intensities were collected at 231 K. Changes are plotted versus time under dark annealing at 236 K. P^{+} signal intensities were determined using EasySpin and SVD analysis (see Supporting Information, Figures S6 and S7).[20] Solid lines are fits of the experimental data to differential equations; $dP^{+}_{1.89}/dt = k_1[P^{+}_{6.54}] - k_3[P^{+}_{1.89}]$, $dP^{+}_{1.81}/dt = k_2[P^{+}_{6.54}] + k_3[P^{+}_{1.89}]$, and $dP^{+}_{6.54}/dt = -(k_1 + k_2)[P^{+}_{6.54}]$ (Table S4). Green, $P^{+}_{6.54}$; blue, $P^{+}_{1.89}$; red, $P^{+}_{1.81}$.

P-cluster intermediate originates together with $P^{+}_{1.89}$ under photochemical reduction of the P^{2+} state (Figure 4). In the dark, $P^{+}_{6.54}$ partitions rapidly between $P^{+}_{1.89}$ or $P^{+}_{1.81}$.

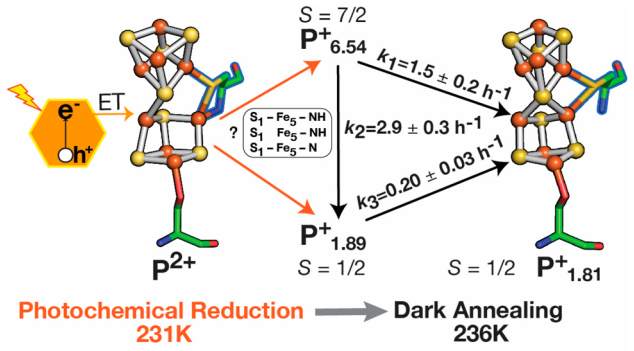

Figure 4. Schematic representation of the P^{2+} to P^{+} conversion in low temperature photochemical reduction of the MoFe protein P-cluster. Photoexcitation at 231 K of CdS:MoFe protein complexes poised in P^{2+} (left) leads to electron injection into the P-cluster and reduction to a mixed population of P^{+} states; the $S = 7/2$ $P^{+}_{6.54}$ and $S = 1/2$ $P^{+}_{1.89}$, which are based on the reaction model (Figure 3), correspond to distinct conformers (inset). Dark annealing at 236 K results in the conversion of $P^{+}_{6.54}$ to either $P^{+}_{1.89}$ (faster) or $P^{+}_{1.81}$ (slower), and conversion of $P^{+}_{1.89}$ to $P^{+}_{1.81}$. The rate constants of the conversion of P^{+} states are obtained from fits shown in Figure 3 to a reaction model in Table S4.

Therefore, a lack of $P^{+}_{6.54}$ under illumination at 263 K (Figure 2) is likely due to more rapid conversion to either $P^{+}_{1.81}$ or $P^{+}_{1.89}$ (k_1 and $k_2 > k_3$) than at 231 K.

Dark annealing was performed over a range of 231 K to 245 K to obtain the temperature-dependence of k_3 for the $P^{+}_{1.89} \leftrightarrow P^{+}_{1.81}$ step (eq 3, Figure S9, Table S6). An Arrhenius plot of ln k_3 vs $1/T$ gave a value of $E_a = 24 \pm 8.3$ kcal mol^{-1}. The value suggests the $P^{+}_{1.89} \leftrightarrow P^{+}_{1.81}$ involves structural changes in MoFe protein at the P-cluster. For example, reductive formation of $P^{+}_{1.81}$ from P^{2+} at 298 K is pH-dependent (Figure 1) and is favored at pH ≈ 6 and nearly undetectable at basic pH (>8).[15] Likewise, chemical oxidation of MoFe protein P-cluster from $P^{N} \leftrightarrow P^{+}$ at 298 K led to formation of both $P^{+}_{1.81}$ and $P^{+}_{1.89}$,[13] with $P^{+}_{1.89}$ intensity being maximal at pH 8.4.[14] The two results are consistent with formation of $P^{+}_{1.89}$ being reversible and both pH- and temperature-dependent.

In addition to analysis of the $P^{+}_{1.89}$ intermediate, photochemical reduction of MoFe protein at 231 K also enabled assignment of the $P^{+}_{6.54}$ high-spin state to a unique electron transfer intermediate (Figure 3). In the $P^{2+} \leftrightarrow P^{+}$ reduction step, the high-spin $P^{+}_{6.54}$ state has two possible fates: direct conversion to $P^{+}_{1.81}$ (eq 3) where $k_2 > k_3$ or rapid conversion to $P^{+}_{1.89}$ followed by slow $P^{+}_{1.89} \leftrightarrow P^{+}_{1.81}$ conversion (eq 2). Thus, the reaction model for the P-cluster $P^{2+} \leftrightarrow P^{+}$ conversion, summarized in Figure 4, involves two spin-state isomer intermediates. The observation of multiple electronic intermediates associated with a redox step in the P-cluster is similar to the observation of low-spin and high-spin S_2 states of the PSII oxygen evolving complex that arise from valence isomerism in Mn−O−Mn coordination from different S_2 conformers that function in the catalytic cycle of water oxidation.[21−25] The interconversion of $P^{+}_{6.54} \leftrightarrow P^{+}_{1.89}$ may likewise arise from conformational isomerism in Fe-coordination to S_1 (see Figure 1) that guide formation of P^{+} with surrounding structural changes. Overall, the results from combining low temperature photochemical reduction of the MoFe protein with dark annealing reveal that formation of the metastable P^{+} state, $P^{+}_{1.81}$, involves intermediate spin states and electronic configurations that occur with changes in P-cluster coordination.

As established by kinetic and theoretical studies, correlated motions within the nitrogenase complex during turnover have an important function in enabling P-cluster mediated electron transfer to be integrated with catalysis.[7−9,26] As shown here, during electron transfer, there are also discrete changes in P-cluster magnetic structure that are linked to changes in oxidation state. The EPR analysis and kinetic model are most consistent with these magnetic states originating from different P-cluster conformers during electron transfer and reduction of P^{2+} to P^{+}, which may function in the electron transfer mechanism within the nitrogenase complex during ammonia production.[27]

■ ASSOCIATED CONTENT

Supporting Information

The Supporting Information is available free of charge at https://pubs.acs.org/doi/10.1021/jacs.1c13311.

A description of experimental procedures including nanocrystal synthesis, EPR spectroscopy and simulation, and reaction models. Figures of parallel mode and low-field perpendicular mode EPR, a detailed analysis for the high-field $P^{+}_{6.54}$ signal assignment, and temperature-

https://doi.org/10.1021/jacs.1c13311
J. Am. Chem. Soc. 2022, 144, 5708−5712

dependence analysis of $P^{+}_{1.89} \leftrightarrow P^{+}_{1.81}$ EPR signals; Tables of spectral analysis and reaction model fits (PDF).

AUTHOR INFORMATION

Corresponding Author

Paul W. King − *Biosciences Center, National Renewable Energy Laboratory, Golden, Colorado 80401, United States; Renewable and Sustainable Energy Institute (RASEI), University of Colorado Boulder, Boulder, Colorado 80309, United States;* orcid.org/0000-0001-5039-654X; Email: paul.king@nrel.gov

Authors

Bryant Chica − *Biosciences Center, National Renewable Energy Laboratory, Golden, Colorado 80401, United States;* orcid.org/0000-0002-6806-4591

Jesse Ruzicka − *Department of Chemistry, University of Colorado Boulder, Boulder, Colorado 80309, United States*

Lauren M. Pellows − *Department of Chemistry, University of Colorado Boulder, Boulder, Colorado 80309, United States;* orcid.org/0000-0002-1088-1898

Hayden Kallas − *Department of Chemistry and Biochemistry, Utah State University, Logan, Utah 84322, United States;* orcid.org/0000-0003-3882-6003

Effie Kisgeropoulos − *Biosciences Center, National Renewable Energy Laboratory, Golden, Colorado 80401, United States*

Gregory E. Vansuch − *Biosciences Center, National Renewable Energy Laboratory, Golden, Colorado 80401, United States*

David W. Mulder − *Biosciences Center, National Renewable Energy Laboratory, Golden, Colorado 80401, United States;* orcid.org/0000-0003-0559-0145

Katherine A. Brown − *Biosciences Center, National Renewable Energy Laboratory, Golden, Colorado 80401, United States;* orcid.org/0000-0001-6060-8294

Drazenka Svedruzic − *Biosciences Center, National Renewable Energy Laboratory, Golden, Colorado 80401, United States;* orcid.org/0000-0002-0229-7229

John W. Peters − *Institute of Biological Chemistry, Washington State University, Pullman, Washington 99163, United States;* orcid.org/0000-0001-9117-9568

Gordana Dukovic − *Department of Chemistry, University of Colorado Boulder, Boulder, Colorado 80309, United States; Renewable and Sustainable Energy Institute (RASEI), University of Colorado Boulder, Boulder, Colorado 80309, United States; Materials Science and Engineering, University of Colorado Boulder, Boulder, Colorado 80303, United States;* orcid.org/0000-0001-5102-0958

Lance C. Seefeldt − *Department of Chemistry and Biochemistry, Utah State University, Logan, Utah 84322, United States;* orcid.org/0000-0002-6457-9504

Complete contact information is available at: https://pubs.acs.org/10.1021/jacs.1c13311

Notes

The authors declare no competing financial interest.

ACKNOWLEDGMENTS

Funding was provided by the U.S. Department of Energy Office of Basic Energy Sciences, Division of Chemical Sciences, Geosciences, and Biosciences, Physical Biosciences and Solar Photochemistry Programs. This work was authored in part by the Alliance for Sustainable Energy, LLC, the manager and operator of the National Renewable Energy Laboratory for the U.S. Department of Energy (DOE) under Contract No. DEAC36-08GO28308. The U.S. Government and the publisher, by accepting the article for publication, acknowledges that the U.S. Government retains a nonexclusive, paid-up, irrevocable, worldwide license to publish or reproduce the published form of this work, or allow others to do so, for U.S. Government purposes.

REFERENCES

(1) Simpson, F. B.; Burris, R. H. A Nitrogen Pressure of 50 atm Does Not Prevent Evolution of Hydrogen by Nitrogenase. *Science* **1984**, *224* (4653), 1095−1097.

(2) Seefeldt, L. C.; Yang, Z.-Y.; Lukoyanov, D. A.; Harris, D. F.; Dean, D. R.; Raugei, S.; Hoffman, B. M. Reduction of Substrates by Nitrogenases. *Chem. Rev.* **2020**, *120* (12), 5082−5106.

(3) Danyal, K.; Dean, D. R.; Hoffman, B. M.; Seefeldt, L. C. Electron Transfer within Nitrogenase: Evidence for a Deficit-Spending Mechanism. *Biochemistry* **2011**, *50* (43), 9255−9263.

(4) Seefeldt, L. C.; Peters, J. W.; Beratan, D. N.; Bothner, B.; Minteer, S. D.; Raugei, S.; Hoffman, B. M. Control of electron transfer in nitrogenase. *Cur. Opin. Chem. Biol.* **2018**, *47*, 54−59.

(5) Peters, J. W.; Stowell, M. H. B.; Soltis, S. M.; Finnegan, M. G.; Johnson, M. K.; Rees, D. C. Redox-Dependent Structural Changes in the Nitrogenase P-Cluster. *Biochemistry* **1997**, *36* (6), 1181−1187.

(6) Keable, S. M.; Zadvornyy, O. A.; Johnson, L. E.; Ginovska, B.; Rasmussen, A. J.; Danyal, K.; Eilers, B. J.; Prussia, G. A.; LeVan, A. X.; Raugei, S.; Seefeldt, L. C.; Peters, J. W. Structural characterization of the P1+ intermediate state of the P-cluster of nitrogenase. *J. Biol. Chem.* **2018**, *293* (25), 9629−9635.

(7) Danyal, K.; Mayweather, D.; Dean, D. R.; Seefeldt, L. C.; Hoffman, B. M. Conformational Gating of Electron Transfer from the Nitrogenase Fe Protein to MoFe Protein. *J. Am. Chem. Soc.* **2010**, *132* (20), 6894−6895.

(8) Huang, Q.; Tokmina-Lukaszewska, M.; Johnson, L. E.; Kallas, H.; Ginovska, B.; Peters, J. W.; Seefeldt, L. C.; Bothner, B.; Raugei, S. Mechanical coupling in the nitrogenase complex. *PLOS Comp. Biol.* **2021**, *17* (3), No. e1008719.

(9) Seefeldt, L. C.; Hoffman, B. M.; Peters, J. W.; Raugei, S.; Beratan, D. N.; Antony, E.; Dean, D. R. Energy Transduction in Nitrogenase. *Acc. Chem. Res.* **2018**, *51* (9), 2179−2186.

(10) Li, Z.; Guo, S.; Sun, Q.; Chan, G. K.-L. Electronic landscape of the P-cluster of nitrogenase as revealed through many-electron quantum wavefunction simulations. *Nat. Chem.* **2019**, *11* (11), 1026−1033.

(11) Pierik, A. J.; Wassink, H.; Haaker, H.; Hagen, W. R. Redox properties and EPR spectroscopy of the P clusters of Azotobacter vinelandii MoFe protein. *Eur. J. Biochem.* **1993**, *212* (1), 51−61.

(12) Chan, J. M.; Christiansen, J.; Dean, D. R.; Seefeldt, L. C. Spectroscopic Evidence for Changes in the Redox State of the Nitrogenase P-Cluster during Turnover. *Biochemistry* **1999**, *38* (18), 5779−5785.

(13) Tittsworth, R. C.; Hales, B. J. Detection of EPR signals assigned to the 1-equiv-oxidized P-clusters of the nitrogenase MoFe-protein from Azotobacter vinelandii. *J. Am. Chem. Soc.* **1993**, *115* (21), 9763−9767.

(14) Siemann, S.; Schneider, K.; Dröttboom, M.; Müller, A. The Fe-only nitrogenase and the Mo nitrogenase from Rhodobacter capsulatus: a comparative study on the redox properties of the metal clusters present in the dinitrogenase components. *Eur. J. Biochem.* **2002**, *269* (6), 1650−1661.

(15) Lanzilotta, W. N.; Christiansen, J.; Dean, D. R.; Seefeldt, L. C. Evidence for Coupled Electron and Proton Transfer in the [8Fe-7S] Cluster of Nitrogenase. *Biochemistry* **1998**, *37* (32), 11376−11384.

(16) Brown, K. A.; Harris, D. F.; Wilker, M. B.; Rasmussen, A.; Khadka, N.; Hamby, H.; Keable, S.; Dukovic, G.; Peters, J. W.; Seefeldt, L. C.; King, P. W. Light-driven dinitrogen reduction

catalyzed by a CdS:nitrogenase MoFe protein biohybrid. *Science* **2016**, *352* (6284), 448−450.
(17) Chica, B.; Ruzicka, J.; Kallas, H.; Mulder, D. W.; Brown, K. A.; Peters, J. W.; Seefeldt, L. C.; Dukovic, G.; King, P. W. Defining Intermediates of Nitrogenase MoFe Protein during N2 Reduction under Photochemical Electron Delivery from CdS Quantum Dots. *J. Am. Chem. Soc.* **2020**, *142* (33), 14324−14330.
(18) Rupnik, K.; Hu, Y.; Lee, C. C.; Wiig, J. A.; Ribbe, M. W.; Hales, B. J. P+ State of Nitrogenase P-Cluster Exhibits Electronic Structure of a [Fe4S4]+ Cluster. *J. Am. Chem. Soc.* **2012**, *134* (33), 13749−13754.
(19) Hagen, W. R. Wide zero field interaction distributions in the high-spin EPR of metalloproteins. *Mol. Phys.* **2007**, *105* (15−16), 2031−2039.
(20) Stoll, S.; Schweiger, A. EasySpin, a comprehensive software package for spectral simulation and analysis in EPR. *J. Magn. Reson.* **2006**, *178* (1), 42−55.
(21) Drosou, M.; Zahariou, G.; Pantazis, D. A. Orientational Jahn-Teller Isomerism in the Dark-Stable State of Nature's Water Oxidase. *Ang. Chem. Int. Ed.* **2021**, *60* (24), 13493−13499.
(22) De Paula, J. C.; Innes, J. B.; Brudvig, G. W. Electron transfer in photosystem II at cryogenic temperatures. *Biochemistry* **1985**, *24* (27), 8114−8120.
(23) Pantazis, D. A.; Ames, W.; Cox, N.; Lubitz, W.; Neese, F. Two interconvertible structures that explain the spectroscopic properties of the oxygen-evolving complex of photosystem II in the S2 state. *Ang. Chem. Int. Ed.* **2012**, *51* (39), 9935−9940.
(24) Vinyard, D. J.; Khan, S.; Askerka, M.; Batista, V. S.; Brudvig, G. W. Energetics of the S2 State Spin Isomers of the Oxygen-Evolving Complex of Photosystem II. *J. Phys. Chem. B* **2017**, *121* (5), 1020−1025.
(25) Zimmermann, J. L.; Rutherford, A. W. Electron paramagnetic resonance properties of the S2 state of the oxygen-evolving complex of photosystem II. *Biochemistry* **1986**, *25* (16), 4609−4615.
(26) Danyal, K.; Rasmussen, A. J.; Keable, S. M.; Inglet, B. S.; Shaw, S.; Zadvornyy, O. A.; Duval, S.; Dean, D. R.; Raugei, S.; Peters, J. W.; Seefeldt, L. C. Fe Protein-Independent Substrate Reduction by Nitrogenase MoFe Protein Variants. *Biochemistry* **2015**, *54* (15), 2456−2462.
(27) Gray, H. B.; Winkler, J. R. Electron flow through metalloproteins. *Biochim. Biophys. Acta (BBA) - Bioenerg.* **2010**, *1797* (9), 1563−1572.

https://doi.org/10.1021/jacs.1c13311
J. Am. Chem. Soc. 2022, 144, 5708−5712